

Microstructure, Morphology, and Lifetime of Armored Bubbles Exposed to Surfactants

Anand Bala Subramaniam, Cecile Mejean, Manouk Abkarian, and Howard A. Stone*

Division of Engineering and Applied Sciences, Harvard University, Pierce Hall, 28 Oxford Street, Cambridge, Massachusetts 02138

Received February 9, 2006. In Final Form: March 21, 2006

We report the behavior of particle-stabilized bubbles (armored bubbles) when exposed to various classes and concentrations of surfactants. The bubbles are nonspherical, which is a signature of the jamming of the particles on the interface, and are stable to dissolution prior to the addition of surfactant. Armored bubbles exposed to surfactants, dissolve, and exhibit distinct morphological, microstructural, and lifetime changes, which correlate with the concentration of surfactant employed. For low concentrations of surfactant, an armored bubble remains nonspherical while dissolving, whereas for concentrations close to and above the surfactant cmc a bubble reverts to a spherical shape before dissolving. We propose a microstructural interpretation, supported by our experimental observations of particle dynamics on the bubble interface, that recognizes the role of interfacial jamming and stresses in particle-stabilization and surfactant-mediated destabilization of armored bubbles.

It is well known that surfactants stabilize foams and emulsions as well as individual bubbles.^{1,2} Also, it has been long recognized that foams and emulsions can be stabilized by colloidal particles,^{3,4} though detailed studies of the particle-enhanced stabilization have been performed only in recent years.⁵ In particular, some cases have been reported where individual bubbles, protected by a close-packed shell of particles (colloidal armor), appear to be stable indefinitely and do not undergo the usual disproportionation.^{6,8}

Nevertheless, many systems contain both particles and surfactants, and a wide variety of responses have been reported.^{5,9} Alargova et al. report that the addition of sodium dodecyl sulfate (SDS), an anionic surfactant, significantly reduced the stability of a foam stabilized by rod-shaped SU-8 particles. (Results were reported at one concentration, 10 wt % SDS, where the primary mode of destabilization was gravity-induced film drainage and foam collapse.⁷) They explain their observations as a consequence of a change in the surface properties of the particles, from hydrophobic to hydrophilic, due to the oriented adsorption of SDS onto the particles. This change decreases the particles' affinity for the interface; consequently, the foam has a lifetime comparable to that of an SDS-stabilized foam.⁷

Here we report on the behavior of individual particle-stabilized bubbles in the presence of surfactant, which is in contrast to Alargova et al.'s original observations of particle-stabilized foams. Indeed, our observations of individual particle-covered bubbles in the absence of surfactant reveal that they adopt nonspherical shapes before stabilizing. These nonspherical bubbles dissolve when exposed to surfactant and exhibit distinct morphological

changes that are dependent on the concentration of surfactant employed. Direct microstructural observations of the particle shell lead us to propose that wetting changes are sufficient to explain destabilization only at relatively high surfactant concentrations, whereas the interfacial stresses on the shell that accompany bubble dissolution play an important role in destabilizing the bubbles for lower surfactant concentrations. Our results provide insights into the open question of the mechanism of particle superstabilization of bubbles in the absence of surfactants and show promise as a novel means of controllably releasing colloidal particles and gases.

In our experiments, we synthesized monodisperse particle-covered bubbles (armored bubbles) through a microfluidic hydrodynamic focusing method¹⁰ or by simply shaking an aqueous suspension of particles to obtain polydisperse bubbles (Experimental Section). Our quantitative experiments were performed with a model suspension of 4.0- μm -diameter surfactant-free charge-stabilized polystyrene particles and the nonionic surfactant Triton X-100. We also conducted qualitative experiments with a variety of particles and surfactant types (anionic and nonionic) to obtain a general overview of the surfactant destabilization phenomenon (Supporting Information). Armored bubbles exposed to cationic surfactants exhibit complicated behavior that is subject to ongoing study.

We place a surfactant-free aqueous sample containing armored bubbles onto a glass slide, and we observe that the buoyant armored bubbles rise to the top of the droplet (Figure 1a). In this configuration, the shell of particles deforms at the bulk air–water interface to produce a distinct flat facet (Figure 1b and c). Our observations indicate that the particles form a bridge between the air phase in the bubble and the atmosphere, with only a thin layer of water in between. Such a bridging effect was shown previously in a system of particle-covered oil droplets.^{11,12} In the case of gas bubbles, the bridging effect that we demonstrate is significant because it allows for the rapid diffusion of gas out of the bubble directly into the atmosphere, through the thin water film.

* Corresponding author. E-mail: has@deas.harvard.edu. Fax: (617) 495-9837.

(1) Adamson, A. W.; Gast, A. P. *Physical Chemistry of Surfaces*, 6th ed.; Wiley: New York, 1997.

(2) Morrison, I. D.; Ross, S. *Colloidal Dispersions: Suspensions, Emulsions, and Foams*; Wiley-Interscience: New York, 2002.

(3) Ramsden, W. *Proc. R. Soc. London* **1903**, *72*, 156–164.

(4) Pickering, S. U. *J. Chem. Soc.* **1907**, 2001.

(5) Binks, B. P. *Curr. Opin. Colloid Interface Sci.* **2002**, *7*, 21–41.

(6) Du, Z.; Bilbao-Montaya, M. P.; Binks, B. P.; Dickinson, E.; Ettelaie, R.; Murray, B. S. *Langmuir* **2003**, *19*, 3106–3108.

(7) Alargova, R. G.; Warhadpande, D. S.; Paunov, V. N.; Velev, O. D. *Langmuir* **2004**, *20*, 10371–10374.

(8) Binks, B. P.; Horozov, T. S. *Angew. Chem., Int. Ed.* **2005**, *44*, 3722–3725.

(9) Aveyard, R.; Binks, B. P.; Fletcher, P. D. I.; Peck, T. G.; Rutherford, C. E. *Adv. Colloid Interface Sci.* **1994**, *48*, 93.

(10) Bala Subramaniam, A.; Abkarian, M.; Stone, H. A. *Nat. Mater.* **2005**, *4*, 553–556.

(11) Ashby, N. P.; Binks, B. P.; Paunov, V. N. *Chem. Commun.* **2004**, 436–437.

(12) Stancik, E. J.; Fuller, G. G. *Langmuir* **2004**, *20*, 4805–4808.

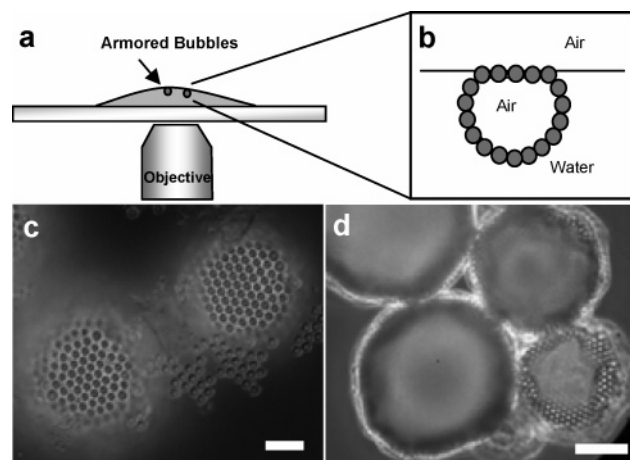


Figure 1. (a) Schematic of the experimental setup. A drop of sample containing the armored bubbles is placed on a slide and visualized from below using an inverted microscope. (b) Buoyant bubbles rise to the surface of the drop and deform to form a facet at the interface. (c) Top view of the armored bubbles taken with an upright microscope. The particles composing the facet are in fact bridging the two air phases, that in the bubble and that in the atmosphere, with an intervening film of water. Scale bar = $16\ \mu\text{m}$. (d) Viewed from below, the bubbles progressively lose gas and take on buckled nonspherical shapes before stabilizing. The ability to sustain nonspherical shapes, as shown here, is a hallmark of solidlike behavior. Scale bar = $48\ \mu\text{m}$.

When viewing through the water phase (i.e., with an inverted microscope), we observe that the bubble progressively takes on a nonspherical shape by losing some gas, after which the nonspherical bubble then remains stable without further changes in volume or shape for at least 2 days (Figure 1d). The observation of buckling and the stable nonspherical shapes suggest that the interface of the armored bubble is behaving in a solidlike manner because equilibrium nonspherical shapes of ordinary bubbles with an isotropic surface tension are prohibited. This solidlike behavior was recently proposed to arise from the jamming of the adsorbed particles on the bubble interface^{10,13,14,15} and is to be contrasted with the apparent maintenance of sphericity in other experiments.⁶

We next systematically investigate the influence of surfactants on the structure and stability of armored bubbles. When a solution of Triton X-100 at a concentration of $c = 0.66\ \text{mM}$ (a critical micelle concentration, cmc, of approximately $0.2\ \text{mM}$) is added to the sample, the nonspherical bubble quickly regains a spherical shape (within one camera frame, or 1 s) by ejecting excess particles from the interface (Figure 2a). The remaining particles on the interface resume Brownian motion in a well-defined hexagonally coordinated lattice. (See movie 1 in Supporting Information where the dynamics of the particles are clearly visible.) The spherical bubble now proceeds to dissolve continuously until it disappears completely (Figure 2a–d, movie 2 in Supporting Information). This observation is reproducible, and generally, armored bubbles with an initial radius of $20\ \mu\text{m}$ take $100 \pm 3\ \text{s}$ to dissolve when exposed to this concentration of surfactant. The response is to be contrasted with the apparent infinite lifetime of an armored bubble in an air-saturated solution and the comparatively shorter lifetime of 50 s for a simple surfactant-covered bubble (Figure 2e).

When Triton X-100 is added at a concentration below the cmc ($0.066\ \text{mM}$) markedly different behavior is observed. The bubble remains nonspherical but starts ejecting particles while losing volume (Figure 3a–d). Moreover, the particles remain immobile on the interface, signifying their still jammed state (movie 3 in Supporting Information). The bubble continues to lose gas with periods of transient stability when the bubble does not change in apparent radius. (Here the apparent radius is taken to be one-half the diagonal length of the smallest bounding rectangle.) Moreover, unlike the case for $c > \text{cmc}$, the lifetimes of individual bubbles are highly variable, ranging from 1190 to 1340 s for bubbles with an initial radius of $20\ \mu\text{m}$ (Figure 3e). Nevertheless, despite the different responses of individual bubbles, all of the bubbles eventually dissolve completely.

We constructed a phase diagram of bubble behavior by exposing individual bubbles to various concentrations of surfactant (Figure 4). The boundary $c_{\text{critical}}^{(2)}$ in the phase diagram, which denotes a change from an aspherical, unstable, jammed shell to a spherical, unstable shell with evident Brownian motion, is not sharply delineated because of the complicated adsorption pattern in these systems. The surfactant adsorbs on the particles and the air–water interface,^{16,17} both of which change in area as the bubble dissolves and particles are ejected, thus preventing the accurate determination of adsorbed amounts and its correspondence to the surfactant cmc. However, we note that this critical concentration is close to the cmc of the surfactants tested, where surfactant adsorption onto surfaces is expected to be maximal.¹⁶

We now seek to rationalize the clear difference in bubble lifetime, microstructure, and morphology, which correlates with surfactant concentration. For $c > c_{\text{critical}}^{(2)}$, the microstructural signature is the unjamming of the shell, and the morphological signature is the rapid return to a spherical shape. Consistent with Alargova et al.'s observations for a different system,⁷ we believe that in this concentration range the surfactant acts as a detergent, promoting the wetting of the particles by adsorbing onto the particles and the air–water interface. Because confinement on an interface is a requirement for interfacial jamming,¹⁰ desorption should lead to the unjamming of the shell. Nevertheless, we note that the morphological and microstructural changes we observe suggest that particle desorption is rapid ($< 1\ \text{s}$) yet the particles remain in a spherical shell-like configuration for the duration of the bubble lifetime (Figure 2). A plausible explanation for this surprising observation is that the surfactant-covered particles, despite being completely wetted by the liquid, experience an attraction to the surfactant-covered air–water interface and thus do not diffuse away. The origin of this long-range attraction remains to be elucidated, though there have been reports of long-range attraction between surfactant-covered surfaces in other systems.¹⁸

The scenario in which the particles are desorbed and remain close to only the interface also accounts for the smooth dissolution profile and the shorter lifetime of the bubbles in the regime of $c > c_{\text{critical}}^{(2)}$ (Figure 2e). The free air–water interface is unable to resist the dissolution of the bubble, and the particles are released when the available surfactant-covered interface decreases as the bubble disappears. Although the particles are not straddling the interface and do not affect the mechanical properties of the interface, the gas-impermeable particles still shield the interface

(13) Bala Subramaniam, A.; Abkarian, M.; Mahadevan, L.; Stone, H. A. *Nature* **2005**, *438*, 930.

(14) Xu, H.; Melle, S.; Golemanov, K.; Fuller, G. G. *Langmuir* **2005**, *21*, 10016–10020.

(15) Stratford, K.; Adhikari, R.; Pagonabarraga, I.; Desplat, C.; Cates, M. E. *Science* **2005**, *309*, 2198–2201.

(16) Rosen, M. J. *Surfactants and Interfacial Phenomena*, 3rd ed.; John Wiley & Sons: Hoboken, NJ, 2004.

(17) Martin-Rodriguez, A.; Cabrerizo-Vilchez, M. A.; Hidalgo-Alvarez, R. J. *Colloid Interface Sci.* **1997**, *187*, 139–147.

(18) Meyer, E. E.; Lin, Q.; Hassenkam, T.; Orudjev, E.; Israelachvili, J. N. *Proc. Natl. Acad. Sci. U.S.A.* **2005**, *102*, 6839–6842.

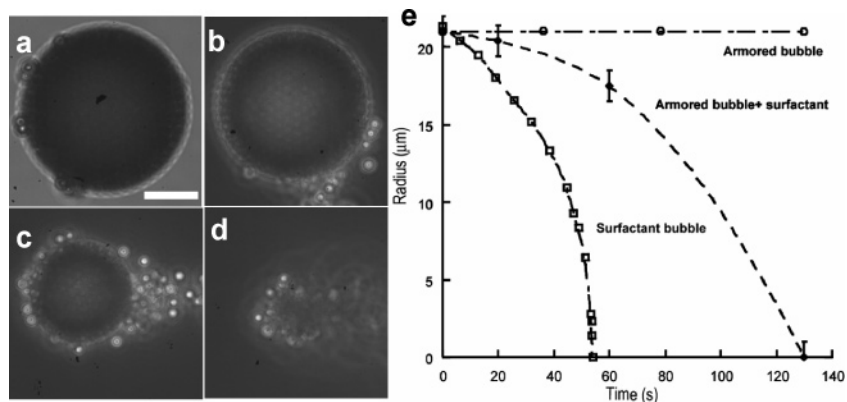


Figure 2. Response of armored bubbles to 0.66 mM Triton X-100 (surfactant); bubbles were covered with polystyrene particles. Scale bar = 24 μm . (a) The initially stable nonspherical bubble regains its spherical shape by rapidly ejecting excess particles from the interface. (b, c) The bubble continues to shed particles smoothly as it decreases in size until (d) it disappears. (e) Radius versus time for a stable armored bubble, an armored bubble exposed to surfactant, and a surfactant-covered bubble under the same experimental conditions. Note that in the presence of surfactant the particles do not halt dissolution but slow it down relative to that of a bare surfactant-covered bubble.

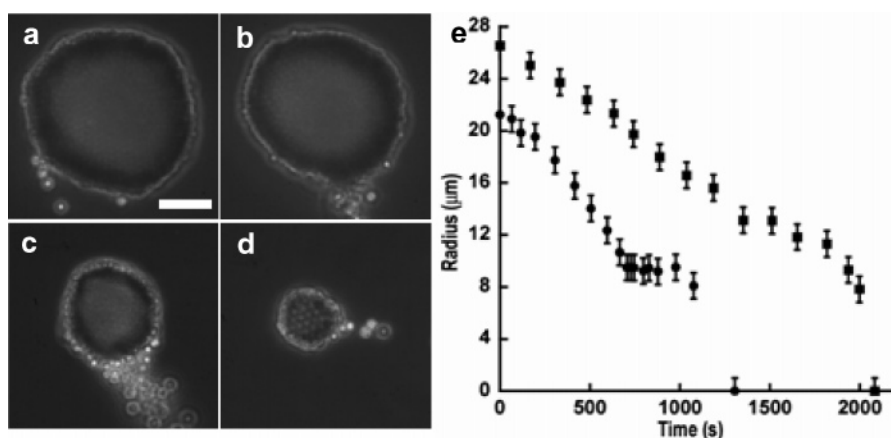


Figure 3. Response of armored bubbles to 0.066 mM Triton X-100. Scale bar = 24 μm . (a, b) The bubble maintains a nonspherical shape but is no longer stable and starts shrinking by losing particles (bright-white circles). (c, d) Nonspherical shape is maintained throughout, until the bubble disappears. (e) Plot of apparent radius (half the diagonal length of the smallest bounding rectangle) versus time of two different armored bubbles exposed to the same experimental conditions. Note that these bubbles take much longer to dissolve compared to those shown in Figure 2 and exhibit transient plateaus where the apparent radius does not change. There is also significant variability in the dissolution time of individual bubbles under similar experimental conditions.

and reduce gas flux out of the dissolving bubble, which is a plausible explanation for the longer lifetime of the armored bubbles exposed to surfactants relative to that of a simple surfactant-covered bubble (Figure 2e).

We next consider the observations for $c < c_{\text{critical}}^{(2)}$ (Figure 3). It is well known that decreasing bulk surfactant concentration results in both smaller changes in wetting properties and surface tension and also an increase in the amount of time required for adsorption.^{1,16} Thus, for a small enough surfactant concentration, no destabilization should occur, which is consistent with our observations for $c < c_{\text{critical}}^{(1)}$, the lowest concentration range reported in the phase diagram (Figure 4). A possible trivial explanation for the longer time scale for destabilization in the intermediate concentration range, $c_{\text{critical}}^{(1)} < c < c_{\text{critical}}^{(2)}$, may be that the surfactant takes a longer time to adsorb onto the particles and causes particle desorption. However, changes in wetting properties do not account for the microstructural and morphological observations of the nonspherical shell (Figures 3 and 4). Moreover, given the significant variability in the lifetime of the bubbles exposed to similar experimental conditions (Figure 3e), we hypothesize that the jamming and the consequent stress-bearing capabilities of the shell might play a role.

A test of our hypothesis requires the untangling of two apparently coupled time scales—the time for surfactant to adsorb

onto the particles and the time for the bubble to shrink. We thus modified the rate of bubble dissolution by placing the bubbles in a semiclosed system, which was a perfusion chamber with two access ports that were left open to the atmosphere (Figure 5). Unlike the experiments performed above, the chamber shields the armored bubbles from direct contact with the atmosphere. The shielding results in a concentration gradient between gas in the bubble and the atmosphere.¹⁹ This causes gas to diffuse from the bubble through the bulk water phase toward the chamber access ports that are at atmospheric pressure. We find that the lifetime of the bubble when exposed to 0.066 mM Triton X-100 is greatly increased to hours from the mere minutes in the open system (Figure 5). During this time, particles desorbed only when the bubbles decreased in size and not otherwise. Because these experiments modify the rate of dissolution and not the time required for surfactant adsorption, it is now clear that the process of gas dissolution is necessary for the ejection of particles from the bubble interface when $c_{\text{critical}}^{(1)} < c < c_{\text{critical}}^{(2)}$.

These observations reveal that the particle shell is providing active rather than passive resistance to the dissolution of the bubble. To illustrate the distinction, consider a balloon composed of a thin elastic membrane: inflating the balloon causes the

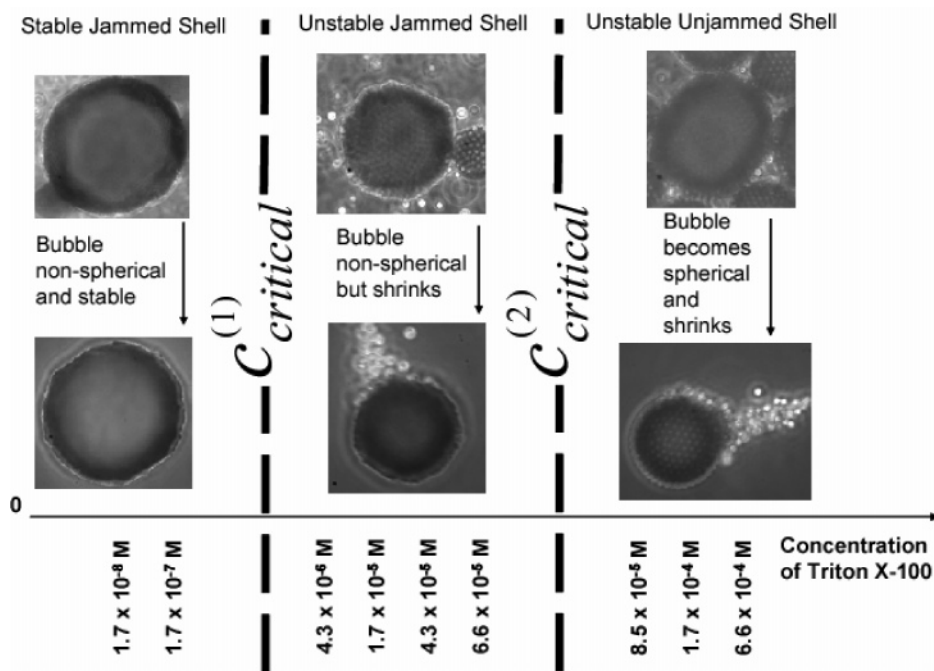


Figure 4. Phase diagram of armored bubble response to surfactant. $c_{critical}^{(1)}$ signifies the critical surfactant concentration above which the armored bubbles are no longer stable to dissolution, and $c_{critical}^{(2)}$ denotes the boundary of the unjamming transition where the particles on the shell resume Brownian motion and the bubble reverts to a sphere. The lifetime of the bubble decreases as the surfactant concentration increases.

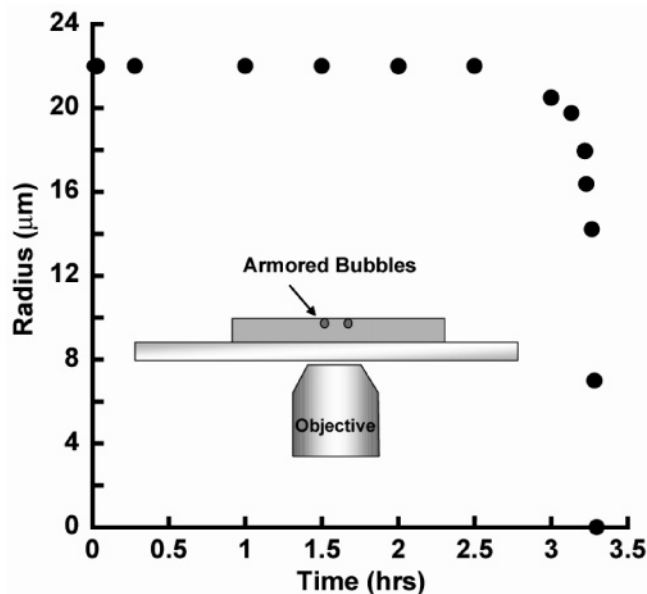


Figure 5. (Inset) schematic of the experimental setup. The bubbles were exposed to 0.066 mM Triton X-100, similar to the concentration employed for the bubbles in Figure 3. Here, the bubbles are kept from direct contact with the atmosphere (compare to Figure 1), thus the gas in the bubble has to diffuse through the bulk fluid phase toward the chamber access ports to equilibrate with the atmosphere. The armored bubble remains stable for about 3 h before beginning to dissolve. No particles are ejected prior to the start of the dissolution process. Note that the time for surfactant diffusion and adsorption should be similar to that in the system open to the atmosphere.

buildup of tensions in the membrane that must resist the internal pressure of the trapped gas. Thus, a blown-up spherical balloon is under higher stress than a deflated one. In contrast, in the case of armored bubbles, the deflation of the bubble due to the dissolution process actually increases the stresses on the shell up to the point where dissolution is halted. A 2D theoretical model by Kam and Rossen of armored bubbles suggests that the

particles might be bearing significant stress that is distributed homogeneously on a spherical shell as the bubble stabilizes.²⁰ The distribution of compressive forces is symmetric in their model, akin to a compression dome, and the consequent rigidity of the shell was suggested to be sufficient to support zero or negative capillary pressures.²⁰ Note, however, that our observation of bubble buckling as gas dissolution occurs suggests that the stress distribution on the bubble surface is not homogeneous (i.e., the shell supports local tensile stresses as well as compressive stresses).

Nevertheless, it appears that the addition of surfactant renders the system unstable, and stressed particles, which otherwise were stably held in the shell, are now ejected to relieve the stress buildup as the bubble shrinks. The inhomogeneities in stress distribution on the jammed shell and the history dependence of particle contact forces for individual bubbles also provide a rational explanation for the nonmonotonic dissolution profile and the varying lifetimes for bubbles when $c_{critical}^{(1)} < c < c_{critical}^{(2)}$ (Figure 3e).

In conclusion, we have shown that isolated particle-stabilized bubbles take on nonspherical shapes as they stabilize. We obtain a general phase diagram of armored bubble behavior versus surfactant concentration and demonstrate that the jammed shell is stressed, a fact that is revealed when the bubble is exposed to surfactant concentrations roughly below the cmc. Because it is apparent that changes in particle wetting are not sufficient to explain particle ejection for $c_{critical}^{(1)} < c < c_{critical}^{(2)}$, the details of surfactant action must be further studied. For concentrations of surfactant close to the cmc, the shell unjams, and the bubble rapidly reverts to a spherical shape. Simple detergency is adequate to explain the lifetime and morphological changes of the bubble in this regime, though the source of the apparent long-range attraction between the bubble and the particles remains to be investigated. The observations we report here have fundamental significance for designing better foam- and bubble-stabilizing technologies.

(20) Kam, S. I.; Rossen, W. R. *J. Colloid Interface Sci.* **1999**, *213*, 329–339.

Experimental Section

We employed 4.0- μm -diameter monodisperse charged-stabilized polystyrene latex particles, 1.6- μm -diameter silica particles (Bangs Lab), 1.0- μm -diameter PMMA particles (Bangs Lab), and polydisperse agglomerated gold microparticles with mean diameters ranging from 1 to 3.99 μm (Sigma). The surfactants used were Triton X-100, sodium dodecyl sulfate (SDS), Tween 20, octyl-B-6-glucopyranoside, and Brij 35, all purchased from Sigma. The cmc of Triton X-100 ranges from 0.22 to 0.5 mM (data from manufacturer). The surfactant solutions were prepared with ultrapure water (Millipore).

An aqueous suspension of particles (10 mL) at a volume fraction of 0.1 was shaken manually and vigorously for about 10 s in a 50 mL test tube. The result was a dilute suspension of gas bubbles, each coated with a jammed shell of particles.

For the experiments open to the atmosphere, we deposited 2.5 μL of the bubble solution onto a glass slide. A particle-free surfactant solution (100 μL) was deposited onto the 2.5 μL sample solution. The large difference in volume was chosen to obtain a homogeneous concentration of surfactant in the entire sample.

We followed the size of the bubbles by capturing pictures with a high-resolution camera. The bubbles were observed using a phase-contrast objective that enhances the contrast of the ejected particles. The bubble diameters were measured within an error of $\pm 1 \mu\text{m}$.

We followed at least three bubbles and repeated the experiment four times for each concentration of surfactant tested. Care was taken to ensure that each system contained only a small number of armored bubbles. Furthermore, the bubble of interest was always isolated from other bubbles by more than 2 times the bubble diameter

in order to avoid multibody effects.²¹ Because the system was exposed to the atmosphere, the concentration of air dissolved in the bulk around each bubble was rapidly equilibrated with atmospheric pressure.

For the experiments in the closed chamber, a Molecular Probes press to seal the perfusion chamber (Molecular Probes) was adhered to a glass slide. The chamber had two access ports at either ends through which the reagents were introduced. We placed 2.5 μL of the bubble solution into the chamber and flushed the chamber with a surfactant solution of known concentration. This ensures that the bubbles are surrounded with liquid of uniform surfactant concentration. The access ports were left open to the atmosphere, and thus gas from the bubble had to diffuse through the bulk fluid phase to equilibrate with atmospheric pressure.¹⁹ All experiments were carried out at room temperature.

Acknowledgment. We thank the Harvard MRSEC and Unilever for support. We also thank D. Gregory and colleagues for helpful conversations.

Supporting Information Available: Movies showing the distinct surfactant-concentration-dependent dynamics of dissolving armored bubbles. Additional experimental data for the various surfactant types employed. This material is available free of charge via the Internet at <http://pubs.acs.org>.

LA060388X

(21) Ettelaie, R.; Dickinson, E.; Du, Z.; Murray, B. S. *J. Colloid Interface Sci.* **2003**, *263*, 47–58.